Paste 2023 – GW Wilson, NA Beier, DC Sego, AB Fourie & D Reid (eds)

doi:10.36487/ACG_repo/2355_07

Determination of the relationship between direct tensile test and Brazilian splitting test of cemented tailings backfill

G Tang *Beijing General Research Institute of Mining and Metallurgy, China*

L Guo *Beijing General Research Institute of Mining and Metallurgy, China*

G Liu *Beijing General Research Institute of Mining and Metallurgy, China*

X Yang *Beijing General Research Institute of Mining and Metallurgy, China*

Abstract

Cemented tailings backfill (CTB) is an artificial structure that provides ground support for the mining structure in the cut-and-fill mining method. The stability of CTB has a bearing on safe and economical production in mines. Tensile strength is an important design parameter that affects the quality of CTB. The Brazilian splitting test (BT) operation is more convenient but the accuracy of results is insufficient. The direct tensile test (DTT), the results of which are accurate though the test threshold is high, can be used to determine the tensile strength of CTB. Therefore, by determining the differences between the results of the two test methods, the tensile strength of CTB can be obtained more precisely using BT. In this study, DTT and BT were performed on CTB with various solid mass contents, binder contents and curing times. The findings demonstrated that, with only numerical differences, the tensile strength of CTB obtained from DTT and BT follows the same pattern of variation with binder content, solid mass content and curing period. The results of BT were lower than those of DTT because the Poisson effect reduces the tensile strength of the BT specimens. A linear fit between the DTT and BT results showed a strong linear correlation with a scale factor of 2.435. This study obtained the scale relationship between the DTT and BT results for the CTB at the test level. The study's findings can serve as a guide for improving the quality assessments and strength designs of CTB in mines.

Keywords: *cemented tailings backfill, tensile strength, direct tensile test, Brazilian splitting test*

1 Introduction

The cut-and-fill mining method, characterised by using backfill to fill in the stopes that have been mined out, makes it possible to safely and economically extract underground mines (Jahanbakhshzadeh et al. 2017; Belem & Benzaazoua 2004). Cemented tailings backfill (CTB) is one of the most common backfill types utilised in cut-and-fill mining, and consists of mine tailings, water and hydraulic binder. These ingredients are first homogeneously mixed to form a slurry which is piped to the underground stopes where it gradually hardens to create CTB (Simon & Grabinsky 2012; Liu et al. 2017; Belem & Benzaazoua 2008). In addition to reducing the surface deposit of solid mine wastes, CTB can also provide regional ground support for stopes (Bull & Fall 2020; Cao et al. 2020).

The work performance of CTB depends on its mechanical properties (Mitchell et al. 1982). Hence, the acquisition of the mechanical properties of CTB has been a significant concern for mining researchers and engineers. The essential design properties of CTB, such as uniaxial compressive strength (UCS), cohesion and the angle of internal friction, can be accurately obtained by uniaxial and triaxial compression tests respectively (Belem et al. 2000; Kesimal et al. 2005; Fall et al. 2007). Tensile strength is also a critical strength property of CTB, but there has still been insufficient research on its determination (Pan & Grabinsky 2021; Guo et al. 2022). Tensile strength affects the quality of CTB in many cases and is further related to the safety of mine production. For example, in the underhand cut-and-fill mining method, miners must work beneath sill mats made of CTB, and the leading cause of damage to the sill mats is insufficient tensile strength (Caceres et al. 2017). Because CTB is brittle it has a lower tensile strength than UCS and is therefore more likely to

crack under tensile stress (Komurlu et al. 2016). Indeed, the tensile strength of CTB must be determined precisely.

Currently, the tensile strength of CTB is typically tested in accordance with the standards and methods for rock or concrete, which are divided into direct and indirect test methods (Chen et al. 2019; Zhou et al. 2021). The direct tensile test (DTT) is a direct test method for determining the tensile strength, and its results are considered representative of the real tensile strength (Fahimifar & Malekpour 2012; Hudson 1969). In DTT, axial tension is applied at both ends of the specimen until the specimen breaks. Assuming that the cross-sectional area of the specimen is constant and that the stress is uniformly distributed over its section, the ratio of the load at fracture to the section's area is the tensile strength of the specimen. Hoek proposed an axisymmetric dog-bone-shaped DTT specimen with an area at each end of the specimen larger than the central cross-section, making it easier to hold and apply tension (Hoek 1964). In addition, there are other DTTs using cylindrical-shaped, 8-shaped or dumbbell-shaped specimens (Bieniawski et al. 1978; Tamrakar et al. 2005; Klanphumeesri 2002). However, two common problems exist in DTTs. Firstly, DTT usually requires a tensile test machine, and special equipment is also necessary for specially shaped specimens. Secondly, DTT specimens are relatively complex-shaped and challenging to make (Mellor & Hawkes 1971; Coviello et al. 2005; Butenuth et al. 1993). Although DTTs are constantly being improved, such as the invention of compression-to-tension load converters (CTLC) and moulds made using 3D printing technology, there are still limitations to the use of DTTs (Pan & Grabinsky 2021; Guo et al. 2022).

The Brazilian splitting test (BT) is an indirect tensile strength test method proposed in 1943 by Carneiro and Akazawa (Carneiro 1943; Akazawa 1943). In this test, a disc specimen is placed in the loading device and the axial direction of the specimen is perpendicular to the direction of the loading. When the specimen is compressed, horizontal tensile stresses are generated in the vertical plane of the specimen where the radial load is applied (Fairhurst 1964). The tensile stress in the central area of the specimen will be the first to reach the specimen's tensile strength. A tensile crack will develop from the central point and expand in a direction perpendicular to the tensile stress, splitting the specimen in half. The tensile strength of the specimen can be calculated from the load applied to the specimen at the time of fracture (Mellor & Hawkes 1971). Compared to DTT, BT is more widely used for testing the tensile strength of rock-like materials. The popularity of the BT is mainly due to the simplicity of specimen production and the convenience of using compression testing equipment for the test (Coviello et al. 2005; Barla & Innaurato 1973). But BT has its drawbacks. According to Griffith's strength theory, the tensile strength measured by BT is valid only if the crack first emerges from the centre of the specimen (Fairhurst 1964). Some studies have shown that the ratio of compressive strength to tensile strength affects the cracking pattern of BT specimens: the higher this ratio, the more likely the specimen is to crack from the centre. The contact area between the specimen and the loading device in BT is narrow and may lead to eccentric tensile cracks in a specimen (Fahimifar & Malekpour 2012). At present, the most common method used in testing the tensile strength of CTB is BT (Yilmaz et al. 2009; Deng et al. 2017; Chen et al. 2019). Nevertheless, CTB is not as brittle as rock or concrete, which influences the accuracy of BT results.

As a result, neither DTT nor BT can achieve accuracy in their results due to the simplicity required for determining the tensile strength of CTB. Therefore, converting the results of the BT to obtain a more practical tensile strength may be a better way. Some studies have obtained a scale factor between the BT results and the theoretical tensile strength using numerical simulations and theoretical calculations (Fahimifar & Malekpour 2012; Yu et al. 2006; Sundaram & Corrales 1980; Yu et al. 2009).

In the work done and reported in the literature, the tensile strength of CTB has been studied mainly by a single test method, and the DTT of CTB has rarely been carried out together with BT. Additionally, the results of analytical calculations and numerical simulations are compared with the results of BT, which are often influenced by theoretical assumptions. In this paper, various backfill mix designs and curing periods were set, taking into account the actual filling conditions in the mine. DTT and BT of CTB were then carried out on the same mix design and curing ages. By comparing the results of the two tests, the relationship between DTT and BT was obtained.

2 Materials and test methods

2.1 Test raw materials

The tailings used in this study were sourced from the Jinchanghe gold mine in Yunnan province, China. The tailings' particle size distribution is depicted in Figure 1. The tailings contained 57.75% of fine fractions less than 38 µm and 75.51% of fine particles less than 74 µm, which are appropriate for making CTB (Zhao et al. 2020). The proportion of tailings with a particle size less than 20 µm is 43%, which exceeds the 15% required for preparing CPB (Sivakugan et al. 2006; Yilmaz et al. 2014).

Table 1 illustrates the chemical characteristics of the tailings. With mass fractions of 34.96%, 25.28% and 21.81%, silicon dioxide (SiO_2), ferric oxide (Fe_2O_3) and calcium oxide (CaO) respectively comprise the majority of the tailings' chemical makeup.

The hydraulic binder was ordinary silicate cement (OPC 42.5), and the water utilised to prepare the specimens was tap water in the area.

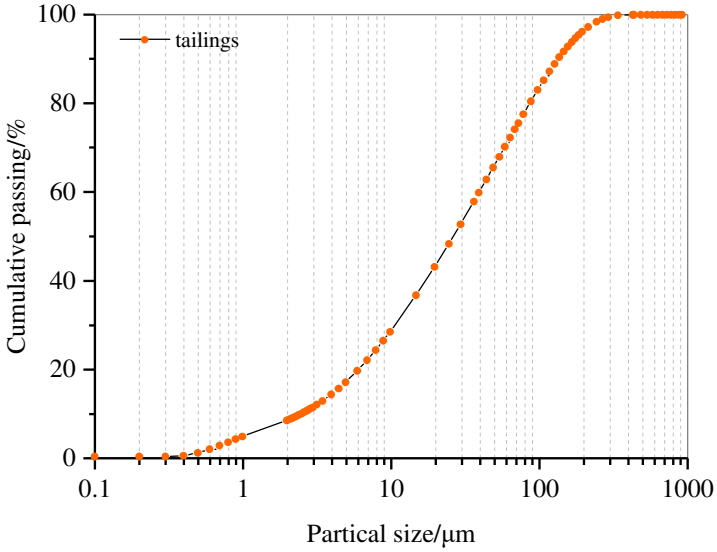

Figure 1 Particle size distribution of tailings

Table 1 The mineralogical composition of tailings

Chemical composition (Wt%)	CaO	SiO_2	Al_2O_3	AgO	Fe_2O_3	P_2O_5	K_2O	Na_2O	SO_3	Other
Tailings	21.81	34.96	1.78	2.47	25.28	0.05	0.37	0.24	0.50	12.53

2.2 Test methods

2.2.1 Mix design and sample preparation

Using combinations of four binder contents and four solid mass contents, 16 mix designs were created, as shown in Table 2. The various designs are shown as S_xB_y, where S_x represents x% of the solid mass content and B_y represents y% of the binder content. $S_{68}B_{9.1}$, for instance, denotes a solid mass content of 68% and a binder content of 9.1%. The CTB with each mix design was cured for 7, 14 and 28 days respectively.

The solid mass content and binder content are defined as Equation 1 and Equation 2:

$$S_C = \frac{m_B + m_T}{m_B + m_T + m_W} \quad (1)$$

$$B_C = \frac{m_B}{m_B + m_T} \quad (2)$$

where:

S_C = solid mass content of the CTB slurry.

B_C = binder content of the CTB slurry.

m_B = mass of the binder.

m_T = mass of the dry tailings.

m_W = mass of the mixing water.

The right quantity of hydraulic binder and tailings were weighed and well mixed before creating the CTB slurry. To create a homogeneous CTB slurry, a predetermined quantity of tap water was added next and stirred with the solid components for at least five minutes. The slurry produced was placed into cylindrical moulds (100 mm height, 50 mm diameter) and dog-bone-shaped moulds with the exact dimensions of Guo's to create specimens for the BT and the DTT (Guo et al. 2022). These slurry-filled moulds were kept in a humidity chamber with a humidity of over 90% and a temperature of 20±0.5°C for the scheduled curing times.

Table 2 Configuration of tensile tests

Solid and binder contend, SxBy	Curing time, t days	DTT test per mix	Number of DT samples	BT test per mix	Number of BT samples
$S_{68}B_{9.1}$	7,14,28	5	15	4	12
$S_{68}B_{11.1}$	7,14,28	5	15	4	12
$S_{68}B_{14.3}$	7,14,28	5	15	4	12
$S_{68}B_{20}$	7,14,28	5	15	4	12
$S_{70}B_{9.1}$	7,14,28	5	15	4	12
$S_{70}B_{11.1}$	7,14,28	5	15	4	12
$S_{70}B_{14.3}$	7,14,28	5	15	4	12
$S_{70}B_{20}$	7,14,28	5	15	4	12
$S_{72}B_{9.1}$	7,14,28	5	15	4	12
$S_{72}B_{11.1}$	7,14,28	5	15	4	12
$S_{72}B_{14.3}$	7,14,28	5	15	4	12
$S_{72}B_{20}$	7,14,28	5	15	4	12
$S_{75}B_{9.1}$	7,14,28	5	15	4	12
$S_{75}B_{11.1}$	7,14,28	5	15	4	12
$S_{75}B_{141.3}$	7,14,28	5	15	4	12
$S_{75}B_{20}$	7,14,28	5	15	4	12

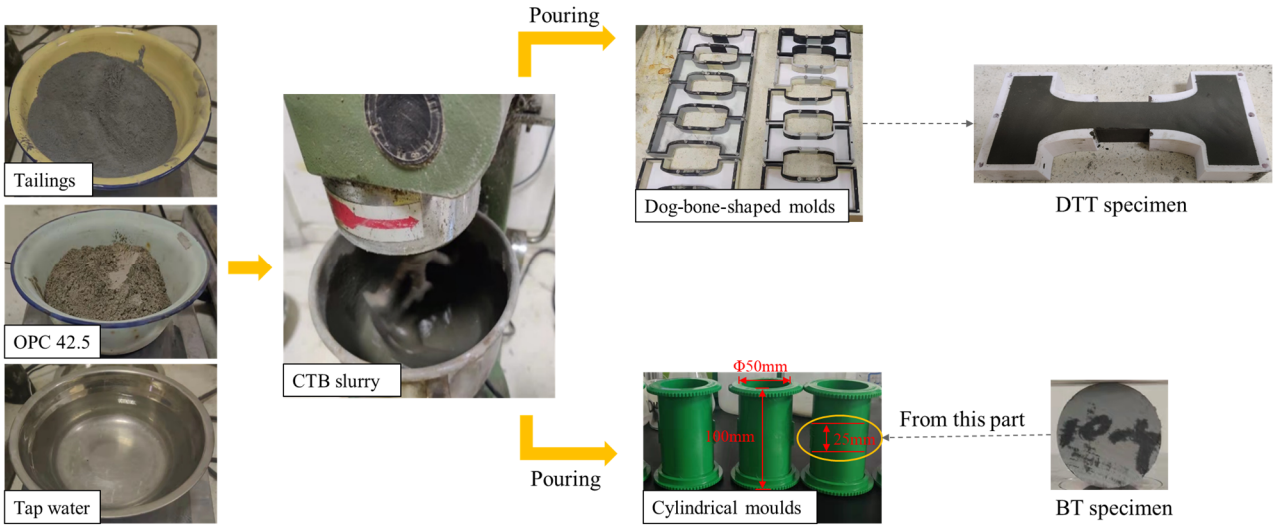

Figure 2 The production process of the CTB specimens

2.2.2 Direct tensile test

Since the introduction of the dog-bone-shaped specimen in the 1960s for tensile strength testing of geotechnical materials, its application and development have continued. In this study, dog-bone-shaped specimens were produced, and DTTs on CTB were carried out in conjunction with Guo's test method (Guo et al. 2022). The tests were performed on a computer-controlled loading machine (HM-5030, Humboldt Mfg. Co., Elgin, IL, USA), and the specimens were stretched using a CTLC device, as shown in Figure 3. The CTLC device secures the upper portion of the specimen while suspending the lower portion. When the CTLC is under pressure, the CTLC applies the load to the lower portion of the specimen and therefore the specimen is stretched. The test's loading rate was maintained at 0.2 mm/min. The specimen's tensile strength is calculated by using the following Equation 3:

$$\sigma_{DT} = \frac{F + 1/2\left(m_s + m_z\right) g}{S} \tag{3}$$

where:

σ_{DT} = tensile strength of the CTB specimen obtained by DTT.

F = failure load pressure.

m_s = weight of the CTB specimen.

m_z = weight of the CTLC.

S = cross-sectional area at the centre of the CTB specimen.

Each mix design with one curing period was a set of tests. Each set of tests was repeated five times to guarantee the reliability of the results. The test result for each set was determined by taking the average of the three results with the smallest dispersion.

Figure 3 Direct tensile test of dog-bone-shaped CTB specimens

2.2.3 Brazilian splitting test

For the BT in this study, disc specimens with a height-to-diameter ratio of 0.5 were utilised in accordance with ASTM D3967 (ASTM 2016). For the purpose of minimising the impact of slurry settlement, each disc specimen was removed from the centre of a cylindrical specimen. The BT was carried out using the same computer-controlled loading machine with DTT and the test apparatus shown in Figure 4, so the load was applied in the radial direction of the specimen. The loader maintained a loading rate of 0.2mm/min until the specimen split. The results of BT were calculated according to Equation 4:

$$\sigma_{BT} = 20 \times \frac{F + mg/1000}{\pi dt} \tag{4}$$

where:

σ_{BT} = tensile strength of the CTB specimen obtained by BT.

F = the failure load pressure.

m = the weight of the upper load device.

d = the diameter of the CTB specimen.

t = the thickness of the CTB specimen.

BT was conducted on four specimens in each set and the result of a set was obtained in the same way described above.

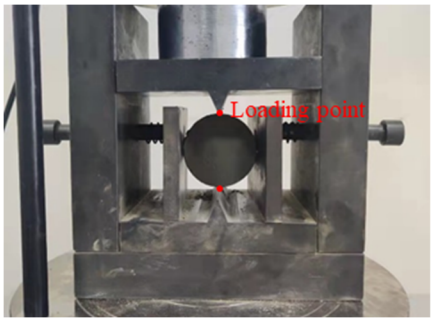

Figure 4 Brazilian splitting test of the disc CTB specimens

3 Results and discussions

3.1 Results of the direct tensile test and the Brazilian splitting test

Figure 5 shows a typical damage pattern of a direct tension specimen where the tensile damage occurred in the middle of the specimen. The tensile section was flat and oriented perpendicular to the direction of tension, indicating that the fracture to the specimen was caused under the tensile stress.

In all of the DTTs, the tensile strength of $S_{68}B_{9.1}$ samples cured for seven days were the only strengths not obtained, due to the fact that their tensile strength was so low that they could fracture under the gravity of the CTLC. For other test results, a partial presentation is made in Figure 7. For example, in Figure 7b, the tensile strengths obtained for specimens with mix design $S_{68}B_{20}$ at the 7-day curing condition were 339.9 kPa, 389.3 kPa, and 379.3 kPa respectively.

Figure 5 Failure pattern of DTT specimens

The disc specimens all split in half along the direction of load application after tests, as illustrated in Figure 6. This is the most typical damage pattern in the BT of CTB (Komurlu 2016). Figure 7 also includes some of the BT data. The tensile strengths of the disc specimens after a 7-day curing period were 154.4 kPa, 139.5 kPa, and 138 kPa, when S_C = 68% and B_C = 20%.

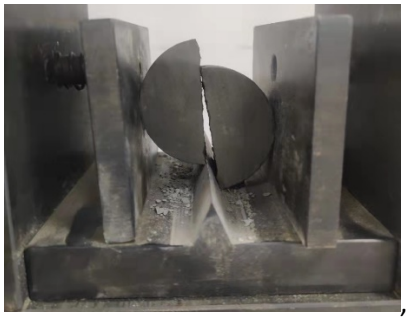

Figure 6 Failure pattern of BT specimens

Additionally, Figure 7 illustrates how the CTB's tensile strength varies with binder content, solid mass content and curing period, as obtained by the two test methods. Overall, the results of the two test methods had the same pattern of variation. The tensile strength of CTB increased linearly with increasing binder content, as shown in Figure 7a. The quantities of hydration products increase in direct proportion to the increase in binder content, which contributes to raising the CTB's strength (Yu 2001).

The growth rate of the tensile strength of CTB is shown in Figure 7b to increase as the solid mass content does. For instance, σ_{DT} at Sc = 68%, 70%, 72% and 75% were 368.3 kPa, 404.6 kPa, 444.6 kPa and 585.2 kPa respectively, and increased by 9.8%, 9.9% and 31.3% in sequence. This is because the increase in solid mass content reduces the sedimentation of tailings particles and the segregation of cement particles, thus improving the quality of the CTB.

Figure 7c shows that the tensile strength of the filler increases more from 7 to 14 days of the curing period than from 14 to 28 days of the curing period, with an increase of 40.0 kPa and 21.7 kPa respectively at these two stages. This is due to the cement hydration reaction being incomplete in the early stages. The hydration products continue to be produced, resulting in a fast increase in tensile strength, while in the later stages, as the unreacted cement content decreases, the hydration reaction rate gradually decreases and the strength growth slows (Nasir & Fall 2008).

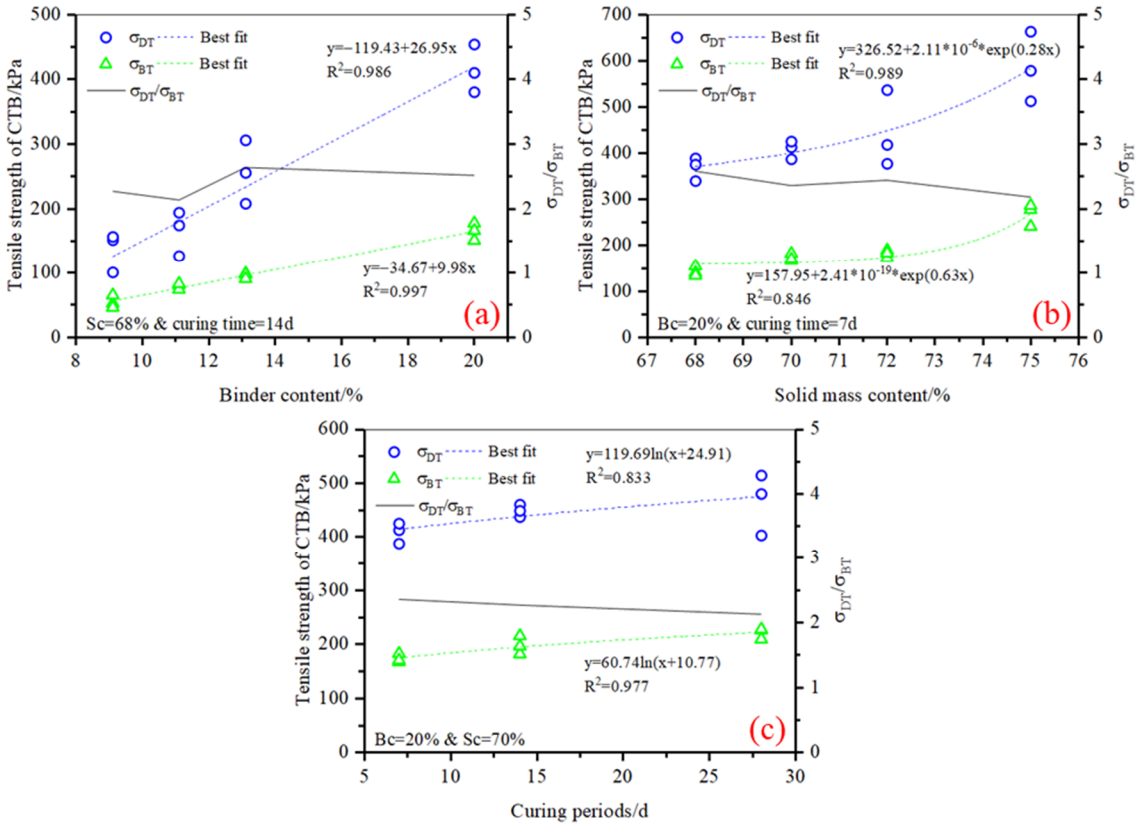

Figure 7 Variation pattern of CTB's tensile strength with different factors: (a) Binder content; (b) Solid mass content; (c) Curing periods

The ratio of the results of the two-test method is also shown in Figure 7. With a ratio between 2 and 3, DTT results are significantly higher than BT.

It is possible that the difference between the results of DTT and BT form the difference in test principles. In BT, the centre of the disc specimen is under a mixed compressive-tensile stress rather than a uniaxial tensile stress (Hondros 1956; Jaeger & Hoskins 1966). The vertical compressive stress increases the tensile strain in the transverse direction of the specimen, thereby reducing its tensile strength (Zhang 1979).

Therefore, the Poisson effect affects the tensile strength obtained by BT. The impact of Poisson's ratio should be considered when comparing the results of BT with the tensile strength obtained by DTT.

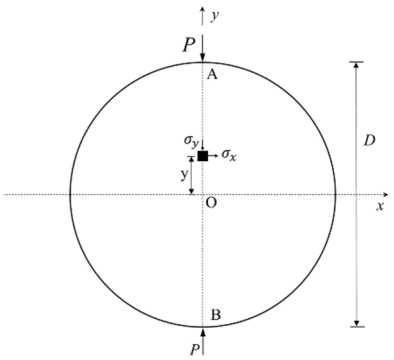

Figure 8 Schematic of the stress distribution on diameter AB in the Brazilian splitting test

Assuming that the mechanical behaviour of the disc specimen conforms to linear elasticity, the horizontal tensile and vertical compressive stresses at the location of the disc diameter AB in the state of force shown in Figure 8 can be expressed respectively by the following equations:

$$\sigma_x = \frac{2P}{\pi DT} \tag{5}$$

$$\sigma_y = -\frac{2P}{\pi DT}\left(\frac{4D^2}{D^2 - 4y^2} - 1\right) \tag{6}$$

where:

σ_x = horizontal tensile stress of the disc.

σ_y = vertical compressive stress of the disc.

P = failure load pressure.

D = diameter of CTB specimen.

T = thickness of CTB specimen.

y = distance from the centre of the disc.

Using the generalised Hooke's law, the strain along the longitudinal centre-line of the disc in the x-direction in the plane stress state ($\sigma_z = 0$) can be deduced as:

$$\varepsilon_x = -\frac{1}{E}\left[\sigma_x - \mu(\sigma_y + \sigma_z)\right] = -\frac{1}{E}(\sigma_x - \mu\sigma_y) \tag{7}$$

where:

ε_x = strain along the x-direction on the longitudinal centre-line of the disc.

E = elastic modulus of the disc.

μ = Poisson's ratio of the disc.

From Equations 5 and 6, the relationship between σ_x and σ_y at the centre of the disc circle is:

$$\sigma_y = -3\sigma_x \tag{8}$$

Substitute σ_y and σ_x in Equation 7 with Equations 8 and 5 respectively:

$$\varepsilon_x = \frac{2P}{\pi EDT}(1+3\mu) \tag{9}$$

Therefore, the tensile strength of the disc specimen is:

$$\sigma_t = \sigma_x = E \cdot \varepsilon_x = \frac{2P}{\pi DT}(1+3\mu) \tag{10}$$

Similarly, the tensile strength of the disc specimen in the plane strain state, taking into account the Poisson effect, can be obtained as:

$$\sigma_t = \frac{2P}{\pi DT}(1+3\mu) \tag{11}$$

Since Poisson's ratio of CTB is between 0.2 and 0.4, the tensile strength calculated using Equations 10 and 11 are 1.6-2.2 and 1.68-2.52 times higher respectively than those calculated using Equation 5, which is the traditional formula of BT. Numerical simulations of BT using specimens with different height-to-diameter ratios and Poisson's ratios have revealed that the tensile strength obtained using the traditional formulae for BT can be up to 40% lower than the theoretical tensile strength (Yu 2005).

Hence, it is normal for the results of BT to be less than the results of DTT. The ratios of the test results obtained in this study did not fall within the range mentioned above, probably because the mechanical behaviour of CTB does not fully conform to the elasticity assumptions in the theoretical analysis and numerical simulations. In addition, the ratio of tensile to compressive elastic modulus also affects the ratio of DTT results to BT results (Yu et al. 2006; Sundaram & Corrales 1980).

3.2 Relationship between DT results and BT results

Figure 9 shows a linear fit between DTT results and BT results for the same mix design and curing period of CTB.

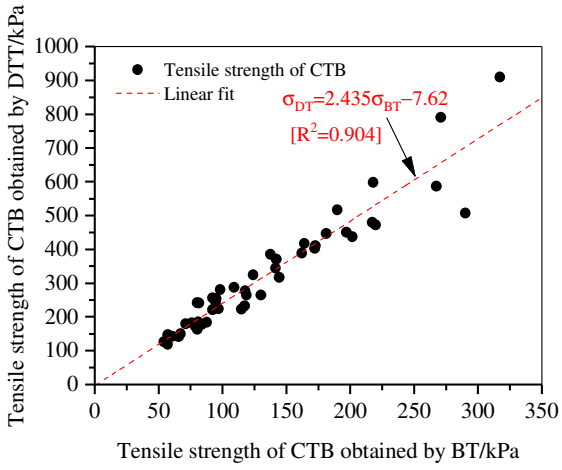

Figure 9 Relationship between the results obtained by DTT and BT

Figure 9 shows that there is a strong linear relationship between the results of the two test methods, with a linear fit equation of:

$$\sigma_{DT} = 2.435\sigma_{BT} - 7.62 \tag{12}$$

Because the intercept of Equation 11 is small relative to the vertical coordinate, the slope of Equation 11 can be considered to be the ratio of DTT strength to the BT strength, i.e. $\sigma_{DT} = 2.435\sigma_{BT}$.

Section 3.1 points out the effect of Poisson's ratio, which is mainly influenced by the binder content of CTB. The higher the binder content, the lower Poisson's ratio of CTB. So this study considers the relationship between the results of two test methods with different binder content, as shown in Figure 10.

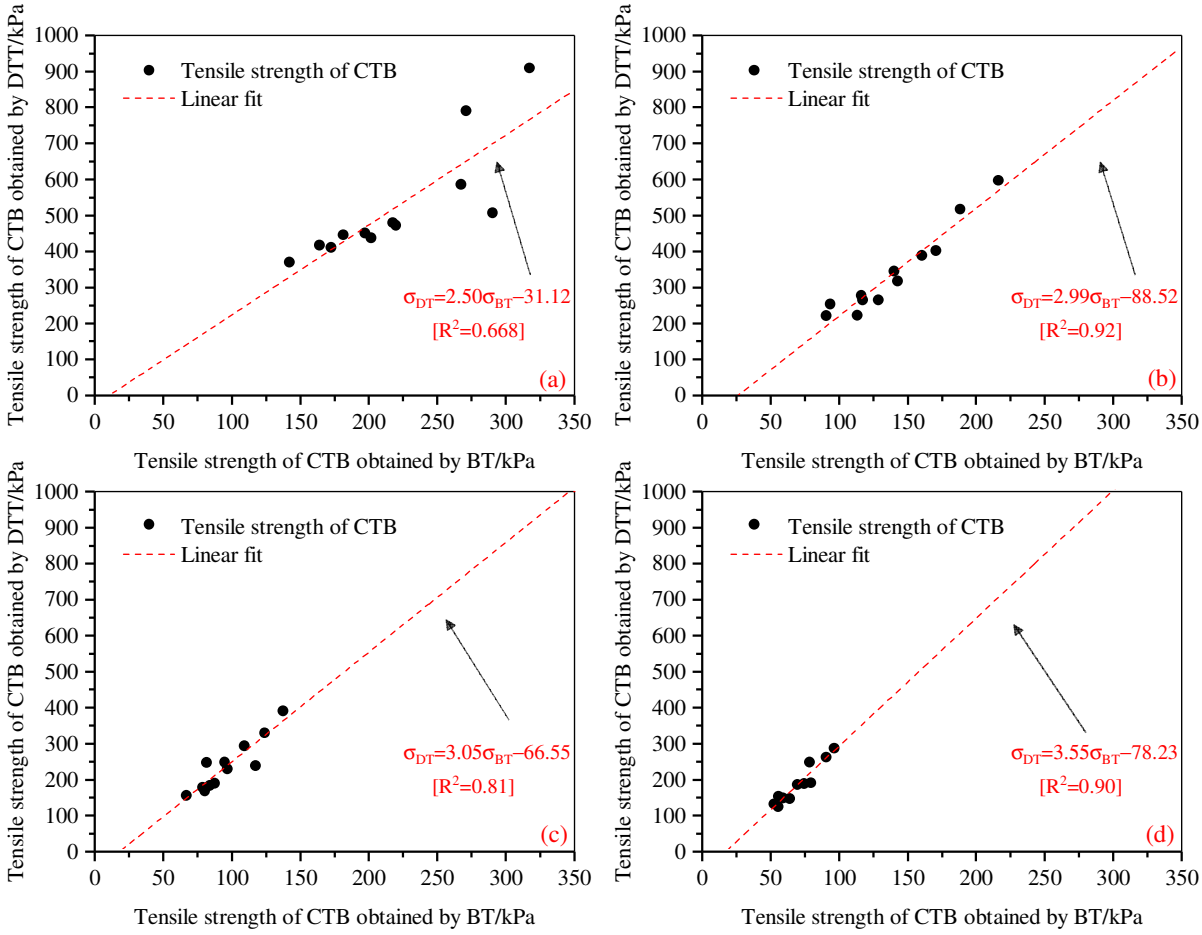

Figure 10 The relationship between results obtained by DTT and BT: (a) Binder content = 20%; (b) Binder content = 14.3%; (c) Binder content = 11.1%; (d) Binder content = 9.1%

The fit results in Figure 10 demonstrate that the slopes of the linear fits increase as the binder content decreases, indicating that the magnitude of the scale factor between the two results increases as Poisson's ratio increases. Equations 9 and 10 as well as the outcomes of the numerical simulation also exhibit the same law, further demonstrating the validity of the test results in this paper and the generality of the variation pattern of the ratio (Yu 2005). When the binder content is low (e.g. Bc = 9.1%), the ratio of compressive strength to tensile strength of CTB is smaller, making the disc specimens less likely to crack at the centre and thus underestimating the tensile strength of the specimens, causing the difference between DTT and BT results to be more pronounced (Qiao et al. 2022; Guo et al. 2022). In Figure 10a, the difference between DTT and BT results is more pronounced when the tensile strength of CTB is higher, but this cannot be considered a general rule by virtue of the current test results. However, when the effect of Poisson's ratio is taken into account separately, its linear fit is not as good as the linear fit of the overall results. Thus the numerical relationship between the two test results, as shown in Figure 9, was obtained through a combination of influences.

It is important to note that for the tests carried out in this paper, both the shape and size of the specimens can have an effect on the results (Van Mier & Van Vliet 2002). The size effect of the BT is well established, whereas the shape and size effects on the direct tensile test of the tailing sand cemented fill used in this paper are not known (Deng et al. 2012). Furthermore, when conducting BT on CTB, it has been demonstrated that the load distribution on the disc specimens can significantly alter the test outcomes (Komurlu et al.

2016). As only one shape and size specimen was used in this study for each DTT and BT, and only one loading method was used in the tests, the ratio of the two test methods' results obtained in this study is not universal.

4 Conclusion

In this study, DTT and BT determined the tensile strength of CTB with 16 mix designs at three curing periods, and the relationship between the results of these two tests was investigated. Following the conducted trials, the following main conclusions can be made:

- Firstly, the results of DTT of CTB followed the same variation pattern as the results of BT concerning binder content, solid mass content and curing period. The tensile strength of CTB increased linearly with the binder content. The growth rate of the tensile strength of CTB increased with increasing solid mass content and decreased with the growing curing period.
- Secondly, the tensile strength of CTB from BT is less than that obtained from DTT. The Poisson effect is one of the reasons for the reduced tensile strength of the BT specimens.
- Thirdly, the results of DTT of CTB showed an overall linear correlation with the results of BT, expressed as $\sigma_{DT} = 2.435\sigma_{BT}$.

In addition, although the relationship between the two test methods' results was determined, the scale factor of 2.435 is only applicable to the study in this paper due to the many factors that affect the results of the tensile test of CTB.

Acknowledgement

Financial support from the National Key Research and Development Program of China (Grant Nos. 2022YFE0129200 & 2021YFC2900600) and the National Nature Fund Project (Grant No. 52274122) is gratefully acknowledged.

References

Akazawa, T 1943, 'New test method for evaluating internal stress due to compression of concrete (the splitting tension test)(part 1)', *Journal of Japan Society of Civil Engineers*, vol. 29, pp. 777–787.

ASTM International 2016, *Standard Test Method for Splitting Tensile Strength of Intact Rock Core Specimens (ASTM 2016 D 3967:2016)*, ASTM International, West Conshohocken.

Barla, G & Innaurato, N 1973, 'Indirect tensile testing of anisotropic rocks', *Rock Mechanics*, vol. 5, no. 4, pp. 215–230.

Belem, T & Benzaazoua, M 2004, 'An overview on the use of paste backfill technology as a ground support method in cut-and-fill mines', in E Villaescusa & Y Potvin (eds), *Proceedings of the 5th International Symposium on Ground Support in Mining and Underground Construction*, A.A. Balkema, Rotterdam, pp. 28–30.

Belem, T & Benzaazoua, M 2008, 'Design and application of underground mine paste backfill technology', *Geotechnical and Geological Engineering*, vol. 26, no. 2, pp. 147–174.

Belem, T, Benzaazoua, M, & Bussière, B 2000, 'Mechanical behaviour of cemented paste backfill', *Proceedings of the 53rd Canadian Geotechnical Conference*, pp. 373–380.

Bieniawski, Z, & Hawkes, I 1978, 'Suggested methods for determining tensile strength of rock materials', *International Journal of Rock Mechanics and Mining Sciences & Geomechanics Abstracts*, vol. 15, no. 3, pp. 99–103.

Bull, AJ & Fall, M 2020, 'Curing temperature dependency of the release of arsenic from cemented paste backfill made with Portland cement', *Journal of Environmental Management*, vol. 269, https://doi.org/10.1016/j.jenvman.2020.110772

Butenuth, C, Freitas, MD, Al-Samahiji D, Park, H, Cosgrove, J & Schetelig, K 1993, 'Observations on the measurement of tensile strength using the hoop test', *International Journal of Rock Mechanics and Mining Sciences & Geomechanics Abstracts*, vol. 30, no. 2, pp. 157–162.

Caceres, C, Moffat, R, & Pakalnis, R 2017, 'Evaluation of flexural failure of sill mats using classical beam theory and numerical models', *International Journal of Rock Mechanics and Mining Sciences*, vol. 99, pp. 21–27.

Cao, S, Xue, G, Song, W & Teng, Q 2020, 'Strain rate effect on dynamic mechanical properties and microstructure of cemented tailings composites', *Construction and Building Materials*, vol. 247.

Carneiro, FLLB 1943, 'A new method to determine the tensile strength of concrete', *Proceedings of the 5th meeting of the Brazilian Association for Technical Rules*, vol. 3, no. 16, pp. 126–129.

Chen, X, Shi, X, Zhou, J & Yu, Z 2019, 'Influence of polypropylene fiber reinforcement on tensile behavior and failure mode of tailings cemented paste backfill', *IEEE Access*, vol. 7, pp. 69015–69026.

Coviello, A, Lagioia, R & Nova, R 2005, 'On the measurement of the tensile strength of soft rocks', *Rock Mechanics and Rock Engineering*, vol. 38, no. 38, pp. 251–273.

Deng, HF, Li, JL, Zhu, M, Wang, RH, Yuan, X, F, & Liu, Q 2012. 'Research on effect of disc thickness-to-diameter ratio on splitting tensile strength of rock'. *Chinese Journal of Rock Mechanics and Engineering*, vol. 31, no. 4, pp.792-798.

Deng, X, Zhang, J, Klein, B, Zhou, N & Dewit, B 2017, 'Experimental characterization of the influence of solid components on the rheological and mechanical properties of cemented paste backfill', *International Journal of Mineral Processing*, vol. 168, pp. 116-125.

Fahimifar, A & Malekpour, M 2012, 'Experimental and numerical analysis of indirect and direct tensile strength using fracture mechanics concepts', *Bulletin of Engineering Geology and the Environment*, vol. 71, no. 2, pp. 269-283.

Fairhurst, C 1964, 'On the validity of the 'Brazilian' test for brittle materials', *International Journal of Rock Mechanics and Mining Sciences & Geomechanics Abstracts*, vol. 1, no. 4, pp. 535–546.

Fall, M, Belem, T, Samb, S & Benzaazoua, M 2007, 'Experimental characterization of the stress–strain behaviour of cemented paste backfill in compression', *Journal of Materials Science*, vol. 42, no. 11, pp. 3914–3922.

Guo, LJ, Peng, XP, Zhao, Y, Liu, GS, Tang, GX & Pan, A 2022, 'Experimental study on direct tensile properties of cemented paste backfill', *Frontiers in Materials*, vol. 9, https://doi.org/10.3389/fmats.2022.864264

Hoek, E 1964, 'Fracture of anisotropic rock', *Journal of the Southern African Institute of Mining and Metallurgy*, vol. 64, no. 10, pp. 501–518.

Hondros, G 1959, 'The evaluation of Poisson's ratio and the modulus of materials of low tensile resistance by the Brazilian (indirect tensile) test with particular reference to concrete', *Australian Journal of Basic and Applied Sciences*, vol. 10, no. 3, pp. 243–268.

Hudson, JA 1969, 'Tensile strength and the ring test', *International Journal of Rock Mechanics and Mining Sciences & Geomechanics Abstracts*, vol. 6, no. 1, pp. 91–97.

Jaeger, JC & Hoskins, ER 1966, 'Rock failure under the confined Brazilian test', *Journal of Geophysical Research*, vol. 71, no. 10, pp. 2651–2659.

Jahanbakhshzadeh, A, Aubertin, M & Li, L 2017, 'A new analytical solution for the stress state in inclined backfilled mine stopes', *Geotechnical and Geological Engineering*, vol. 120, no. 3, pp. 1151–1167.

Kesimal, A, Yilmaz, E, Ercikdi, B, Alp, I & Deveci, H 2005, 'Effect of properties of tailings and binder on the short-and long-term strength and stability of cemented paste backfill', *Materials Letters*, vol. 59, no. 28, pp. 3703–3709.

Klanphumeesri, S 2002, 'Direct tension testing of rock specimens', master's thesis, Suranaree University of Technology, Suranaree**.**

Komurlu, E, Kesimal, A & Demir, S 2016, 'Experimental and numerical analyses on determination of indirect (splitting) tensile strength of cemented paste backfill materials under different loading apparatus', *Geomechanics and Engineering*, vol. 10, no. 6, pp. 775–791.

Liu, G, Li, L, Yao, M, Landry, D, Malek, F, Yang, X & Guo, L 2017, 'An investigation of the uniaxial compressive strength of a cemented hydraulic backfill made of alluvial sand', *Minerals*, vol. 7, no. 1, p. 4.

Mellor, M & Hawkes, I 1971, 'Measurement of tensile strength by diametral compression of discs and annuli', *Engineering Geology*, vol. 5, no. 3, pp. 173–225.

Mitchell, RJ, Olsen, RS, & Smith, JD 1982, 'Model studies on cemented tailings used in mine backfill', *Canadian Geotechnical Journal*, vol. 19, no. 1, pp. 14–28.

Nasir, O & Fall, M 2008, 'Shear behaviour of cemented pastefill-rock interfaces', *Engineering Geology*, vol. 101, no. 3–4, pp. 146–153.

Pan, A & Grabinsky, MW 2021, 'Tensile strength of cemented paste backfill', *Geotechnical Testing Journal*, vol. 44, no. 6, pp. 1886–1897.

Qiao, L, Li, Q & Zhao, G 2022, 'Numerical study of the Brazilian tensile test: 2D and 3D simulations', *Chinese Journal of Engineering*, vol. 44, no. 1, pp. 131–142.

Simon, D & Grabinsky, MW 2012, 'Electromagnetic wave-based measurement techniques to study the role of Portland cement hydration in cemented paste backfill materials', *International Journal of Mining, Reclamation and Environment*, vol. 26, no. 3, pp. 3–28.

Sivakugan, N, Rankine, RM, Rankine, KJ & Rankine, KS 2006, 'Geotechnical considerations in mine backfilling in Australia', *Journal of Cleaner Production*, vol. 14, no. 12–13, pp. 1168–1175.

Sundaram, PN & Corrales, JM 1980, 'Brazilian tensile strength of rocks with different elastic properties in tension and compression', *International Journal of Rock Mechanics and Mining Sciences & Geomechanics Abstracts*, vol. 17, no. 2, pp. 131–133.

Tamrakar, SB, Toyosawa, Y & Itoh, K 2005, 'Tensile strength of soil measured using newly developed tensile strength apparatus', *Research Reports of National Institute of Industrial Safety*, vol. 2004, pp. 41–51.

Van Mier, JGM & Van Vliet, MRA 2002, 'Uniaxial tension test for the determination of fracture parameters of concrete: state of the art', *Engineering Fracture Mechanics*, vol. 69, no. 2, pp. 235–247.

Yilmaz, E, Benzaazoua, M, Belem, T & Bussière, B 2009, 'Effect of curing under pressure on compressive strength development of cemented paste backfill', *Minerals Engineering*, vol. 22, no. 9–10, pp. 772–785.

Yılmaz, T, Ercikdi, B, Karaman, K & Külekçi, G 2014, 'Assessment of strength properties of cemented paste backfill by ultrasonic pulse velocity test', *Ultrasonics*, vol. 54, no. 5, pp. 1386–1394.

Yu, B 2001, 'Analysis of factors to affect the strength of cemented tailings grain fillings', *Heibei Metallugry,* vol. 3, pp. 3–6.

Yu, Y 2005, 'Questioning the validity of the Brazilian test for determining tensile strength of rocks', *Yanshilixue Yu Gongcheng Xuebao/Chinese Journal of Rock Mechanics and Engineering*, vol. 24, no. 7, pp. 1150–1157.

Yu, Y, Yin, J & Zhong, Z 2006, 'Shape effects in the Brazilian tensile strength test and a 3D FEM correction', *International journal of rock mechanics and mining sciences*, vol. 43, no. 4, pp. 623–627.

Yu, Y, Zhang, J & Zhang, J 2009, 'A modified Brazilian disk tension test', *International journal of rock mechanics and mining sciences*, vol. 46, no. 2, pp. 421–425.

Zhang, S 1979, 'Theoretical relationship and test comparison between splitting tensile strength and axial tensile strength of concrete', *Journal of Changsha Railway University*, vol. 2, pp. 65–82+199.

Zhao, Y, Taheri, A, Karakus, M, Chen, Z & Deng, A 2020, 'Effects of water content, water type and temperature on the rheological behaviour of slag-cement and fly ash-cement paste backfill', *International Journal of Mining Science and Technology*, vol. 30, no. 3, pp. 271–278.

Zhou, Y, Yan, Y, Zhao, K, Yu, X, Song, Y, Wang, J & Suo, T 2021, 'Study of the effect of loading modes on the acoustic emission fractal and damage characteristics of cemented paste backfill', *Construction and Building Materials*, vol. 277, https://doi.org/10.1016/j.conbuildmat.2021.122311